Accepted Manuscript

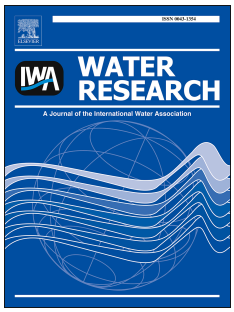

Low pressure UV/H_2O_2 treatment for the degradation of the pesticides metaldehyde, clopyralid and mecoprop – kinetics and reaction product formation

Sofia Semitsoglou-Tsiapou, Michael R. Templeton, Nigel J.D. Graham, Lucía Hernández Leal, Bram J. Martijn, Alan Royce, Joop C. Kruithof

PII: S0043-1354(16)30017-3

DOI: 10.1016/j.watres.2016.01.017

Reference: WR 11771

To appear in: *Water Research*

Received Date: 19 September 2015

Revised Date: 19 December 2015

Accepted Date: 9 January 2016

Please cite this article as: Semitsoglou-Tsiapou, S., Templeton, M.R., Graham, N.J.D., Hernández Leal, L., Martijn, B.J., Royce, A., Kruithof, J.C., Low pressure UV/H_2O_2 treatment for the degradation of the pesticides metaldehyde, clopyralid and mecoprop – kinetics and reaction product formation, *Water Research* (2016), doi: 10.1016/j.watres.2016.01.017.

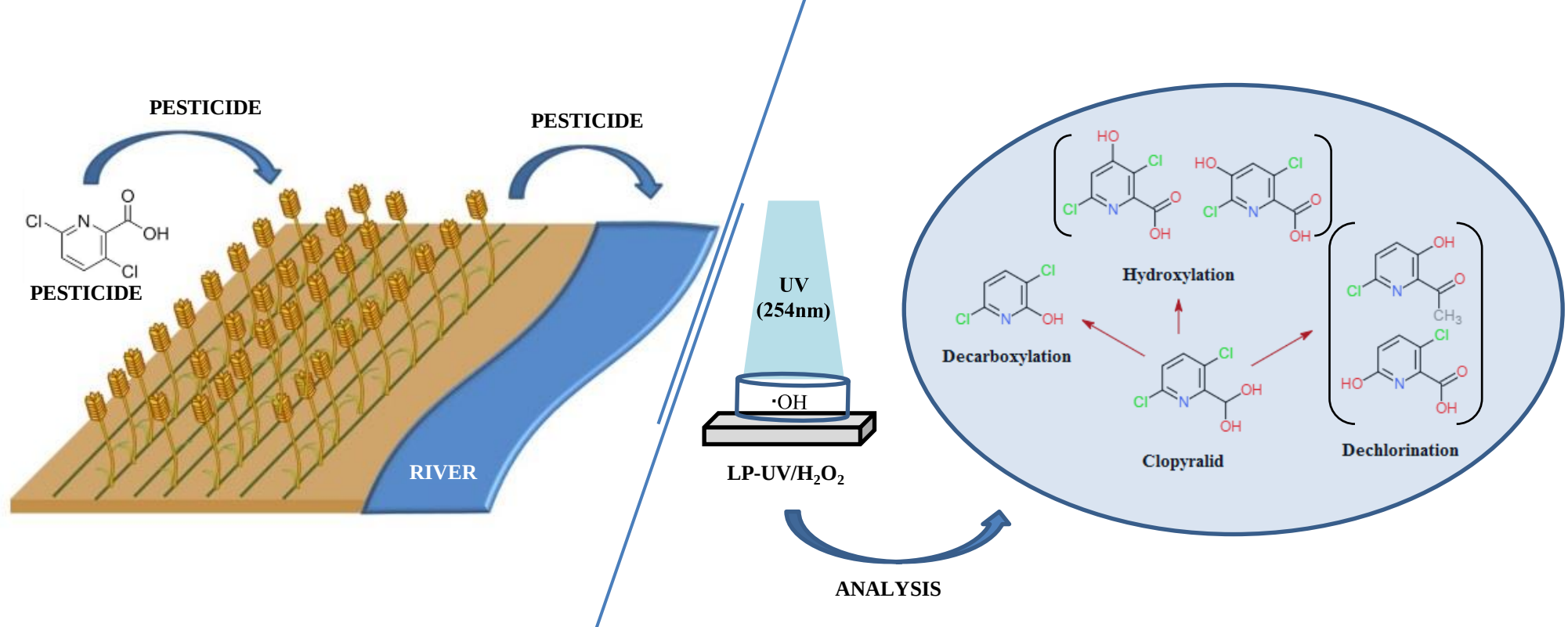
PESTICIDE
PESTICIDE
PESTICIDE
RIVER
UV
(254nm)
·OH
LP-UV/H2O2
Hydroxylation
Decarboxylation
Clopyralid
Dechlorination
ANALYSIS

Low pressure UV/H_2O_2 treatment for the degradation of the pesticides metaldehyde, clopyralid and mecoprop – kinetics and reaction product formation

Sofia Semitsoglou-Tsiapou[a,b,1], Michael R. Templeton[a], Nigel J.D. Graham[a], Lucía Hernández Leal[b], Bram J. Martijn[c], Alan Royce[d], Joop C. Kruithof[b]

[a]Department of Civil and Environmental Engineering, Imperial College London, London, UK

[b]Wetsus, European centre of excellence for sustainable water technology, Leeuwarden, the Netherlands

[c]PWN Technologies, Velserbroek, The Netherlands

[d]Trojan Technologies, London, Ontario Canada

Keywords

Metaldehyde, Clopyralid, Mecoprop, LP-UV/H_2O_2, Kinetics, Reaction products

Abstract

[1] Corresponding author: s.semitsoglou-tsiapou12@imperial.ac.uk, tel.+310628468606, PO Box 1113, 8900 CC, Leeuwarden

The degradation kinetics of three pesticides - metaldehyde, clopyralid and mecoprop - by ultraviolet photolysis and hydroxyl radical oxidation by low pressure ultraviolet hydrogen peroxide (LP-UV/H_2O_2) advanced oxidation was determined. Mecoprop was susceptible to both LP-UV photolysis and hydroxyl radical oxidation, and exhibited the fastest degradation kinetics, achieving 99.6% (2.4-log) degradation with a UV fluence of 800 mJ/cm^2 and 5 mg/L hydrogen peroxide. Metaldehyde was poorly degraded by LP-UV photolysis while 97.7% (1.6-log) degradation was achieved with LP-UV/H_2O_2 treatment at the maximum tested UV fluence of 1000 mJ/cm^2 and 15 mg/L hydrogen peroxide. Clopyralid was hardly susceptible to LP-UV photolysis and exhibited the lowest degradation by LP-UV/H_2O_2 among the three pesticides. The second-order reaction rate constants for the reactions between the pesticides and OH-radicals were calculated applying a kinetic model for LP-UV/H_2O_2 treatment to be $3.6x10^8$, $2.0x10^8$ and $1.1x10^9 M^{-1} s^{-1}$ for metaldehyde, clopyralid and mecoprop, respectively. The main LP-UV photolysis reaction product from mecoprop was 2-(4-hydroxy-2-methylphenoxy) propanoic acid, while photo-oxidation by LP-UV/H_2O_2 treatment formed several oxidation products. The photo-oxidation of clopyralid involved either hydroxylation or dechlorination of the ring, while metaldehyde underwent hydroxylation and produced acetic acid as

40 a major end product. Based on the findings, degradation pathways
41 for the three pesticides by LP-UV/H_2O_2 treatment were proposed.

42 1. Introduction

43 Many pesticides are chemically stable, toxic, and non-
44 biodegradable and may be resistant to direct decomposition by
45 sunlight (Gill and Garg, 2014). Therefore, pesticide residues persist
46 in the environment and pose a risk to both ecosystems and human
47 health. Although water treatment processes such as granular
48 activated carbon (GAC) filtration and/or ozonation are effective
49 barriers for the removal and degradation of many pesticides, in
50 particular clopyralid and metaldehyde are not readily removed by
51 such technologies because of their polarity and chemical structure
52 (Cooper 2011). For this reason, advanced oxidation processes
53 (AOPs) are considered to treat water containing these contaminants
54 (Swaim et al. 2008, Vilhunen and Sillanpää 2010).

55 This study focused on three pesticides, metaldehyde, clopyralid
56 and mecoprop because of their differences in susceptibility to
57 degradation by LP-UV photolysis and hydroxyl radical oxidation,
58 their presence in European water bodies and the scarce information
59 on their degradation by low pressure (LP)-UV/H_2O_2 AOP in
60 literature, especially for clopyralid and metaldehyde. The

61 structures of these pesticides are shown in Figure 1 and their
62 physicochemical characteristics are given in Table S1.

63 Mecoprop ((R,S) 2-(2-methyl-4-chlorophenoxy)-propionic acid), a
64 chlorophenoxy herbicide, developed circa 1956, is commonly
65 applied to control a variety of weeds and is found in groundwater
66 wells and abstractions in many areas around Europe (University of
67 Hertfordshire 2015). Clopyralid (3,6-dichloro-2-pyridine-
68 carboxylic acid) is used to control broadleaf weeds in certain crops
69 and turf. Its chemical stability along with its mobility enables
70 penetration through the soil, causing long term contamination of
71 groundwater as well as surface water supplies (Tizaoui et al. 2011).
72 Both mecoprop and clopyralid are frequently detected in drinking
73 water (Donald et al. 2007). Metaldehyde (2,4,6,8-tetramethyl-
74 1,3,5,7-tetraoxocane) is a contact and systemic molluscicide bait
75 for controlling slugs and snails. In 2009, the UK Drinking Water
76 Inspectorate (DWI) Annual Reports for drinking water quality in
77 England and Wales reported that metaldehyde was responsible for
78 one third of the 1103 water quality failures, since it is not removed
79 by GAC -filtration or degraded by ozonation (Drinking Water
80 Inspectorate 2015).

81 The treatability of these pesticides by various AOPs has been
82 investigated previously but no studies have been reported so far

concerning OH-radical assisted oxidation by LP-UV/H_2O_2 treatment. Meunier and Boule (2000) and Boule et al. (2002) studied the photo-transformation of aromatic pesticides, including mecoprop. They reported that the photo-transformation of mecoprop yielding a number of photo-products, mainly by heterolytic photo-hydrolysis was pH-dependent and was not influenced by oxygen or UV light in the wavelength range of 254-310 nm. Sojic et al. (2009) proposed pathways of clopyralid degradation by medium pressure (MP)-UV/TiO_2 treatment suggesting radical reactions and hydroxylation of the ring, whereas Xu et al. (2013) applied MP-UV/H_2O_2 treatment resulting in dechlorination and formation of further oxidation products. Topalov et al. (1999) studied mecoprop degradation by MP-UV/TiO_2 treatment and proposed radical reactions resulting into a hydroxylated/dechlorinated aromatic moiety and acetic acid as the main products. Autin et al (2012) reported on the degradation of metaldehyde by LP-UV/H_2O_2 and LP- UV/TiO_2 treatment but did not include any details of reaction product formation. Moriarty et al. (2003) proposed mechanisms for the reaction of cyclic ethers with OH-radicals that could apply to metaldehyde as well.

The aim of this study was to investigate the suitability of the LP-UV/H_2O_2 AOP for the degradation of the three selected compounds by evaluating the comparative degradation kinetics for

LP-UV photolysis and hydroxyl radical oxidation, the formation of the major reaction products and the possible reaction pathways for their formation.

2. Materials and Methods

2.1 Chemicals

Metaldehyde, clopyralid, mecoprop, 4-chlorobenzoic acid (pCBA) and bovine catalase were purchased from Sigma-Aldrich (Zwijndrecht, The Netherlands). Sodium dihydrogen phosphate, disodium hydrogen phosphate, hydrogen peroxide (30%) and HPLC-grade methanol (99.9%), the latter used for analytical purposes, were purchased from VWR (Leuven, Belgium). Laboratory grade water (LGW) was produced by a Milli-Q Advantage A10 system (Merck Millipore, Darmstadt, Germany).

Stock and working solutions for all experiments were prepared in Milli-Q water. The stock solutions were prepared by adding the pesticide, followed by moderate heating and sonication if needed, to achieve complete dissolution.

2.2 UV Collimated Beam Experiments

UV exposure experiments were carried out with a bench scale collimated beam apparatus, equipped with a 25 Watt low pressure

126 mercury arc discharge lamp without a lamp sleeve. The emission
127 spectrum of the UV lamp, obtained from Trojan UV Technologies
128 (London, Ontario, Canada) mainly consisted of a strong emission
129 at 254 nm. A warm-up time of at least 20 min was allowed to
130 ensure a constant light output before irradiating the solution. A
131 sample volume of 55 mL was placed in a Petri dish and H_2O_2 was
132 added to obtain the desired concentration. The distance between
133 the lamp and the surface of the sample was 29.5 cm. As soon as the
134 sample was placed under the collimating tube, mixing was started,
135 and the irradiation time was measured as soon as the shutter was
136 opened. Immediately after irradiation, H_2O_2 was quenched with the
137 addition of bovine catalase, the samples were filtered (0.45μm pore
138 size) and stored in the dark at 4°C until analysis.

139 The fluence rate in the center of the sample was 0.2 mW/cm^2 and
140 the path length through the sample solution was 1.96 cm. The
141 Petri Factor was measured before every batch of daily experiments
142 by measuring the fluence rate across the x–y surface using a
143 radiometer and was equal to 0.96 (ILT1700 Radiometer, LOT-
144 QuantumDesign GmbH, USA). The absorption spectra of the three
145 pesticides in the UV region (Figure S1), and the absorbance of the
146 water samples at 254 nm, were used to calculate the exposure time
147 for the desired UV fluences, using a fluence calculation
148 spreadsheet based on Bolton and Linden (2003).

149 Single-solute experiments were performed in Milli-Q water. For
150 the kinetic experiments the initial pesticide concentration was 0.3
151 mg/L, in order to exceed the analytical detection limit, being at the
152 same time as close as possible to realistic concentrations of these
153 compounds in surface water. UV fluences in the range of 0-1000
154 mJ/cm^2, in steps of 200 mJ/cm^2, and H_2O_2 doses of 0, 5 and 15
155 mg/L were applied. Irradiation times ranged from 30 to 90 min,
156 with larger times corresponding to higher UV fluences. The
157 solutions were not buffered but pH was monitored and variations
158 were within 1 pH unit (6.5-7.2).

159 Competition kinetics experiments for the determination of the
160 second-order rate constants between the pesticides and the OH-
161 radicals were conducted in laboratory grade water spiked with 1
162 mg/L of each compound and 0.5 mg/L of pCBA as a hydroxyl
163 radical probe compound. The samples were irradiated with a range
164 of UV fluences 200-500 mJ/cm^2 in steps of 100 mJ/cm^2 and 5
165 mg/L of H_2O_2 as the source of the OH-radicals.

166 For the reaction product formation experiments, the initial
167 concentrations, UV fluences and H_2O_2 doses were increased
168 compared to those for the kinetics experiments, in order to achieve
169 formation of reaction products at quantifiable levels and determine
170 their profiles with UV fluence (reaction time). The initial

concentrations were 5 mg/L for metaldehyde, 10 mg/L for mecoprop and 20 mg/L for clopyralid. The UV fluences were 0-1500 mJ/cm^2, applied in steps of 500 mJ/cm^2 for all three pesticides. The H_2O_2 doses were 10 and 30 mg/L for metaldehyde and mecoprop, and 10, 30 and 60 mg/L for clopyralid. For mecoprop, LP-UV photolysis experiments (no H_2O_2) were performed as well, since it is the only photo-labile compound of the three. All samples were buffered at pH 8 with a phosphate buffer solution. Before analysis, the peroxide was quenched, with the addition of bovine catalase (except for Total Organic Carbon (TOC) analysis), the samples were filtered (0.45µm) and stored in the dark at 4°C until analysis. All experiments were performed in duplicate.

2.3 Analytical Methods

The pesticides (metaldehyde, clopyralid, mecoprop) and p-chlorobenzoic acid were detected and quantified in each sample by liquid chromatography tandem mass spectrometry (LC-MS/MS) using an Agilent 6410 QQQ Mass Analyzer with electrospray ion source. Metaldehyde was detected in the positive mode, whereas clopyralid, mecoprop and p-chlorobenzoic acid were detected in the negative mode. A Phenomenex Kinetex Phenyl-Hexyl column (100mm*2.1mm, 2.6µm particle size) was used, equipped with an

appropriate guard column. The mobile phases used for the positive mode were A: 2.5 L Milli-Q water with 2 mL formic acid (99%) and 1 mL ammonia (30%), and B: 2.5 L acetonitrile with 0.1% formic acid, and for the negative mode A: 2.5 L Milli-Q water with 0.75 mL formic acid (99%) and 1.5 mL ammonia (30%), and B: 2.5 L acetonitrile. The flow rate was 0.35 mL/min. As internal standards, fenoprofen for the negative mode and dihydrocarbamazepine for the positive method were used. For instrument control and data analysis Agilent Masshunter Quant software was used. The same method was used for the detection of the reaction products from each pesticide. Before every set of experiments, calibration curves (0.5-1000 µg/L) for the pesticides were generated with good linearity (R^2>0.99).

The chloride ion was quantified in each sample by ion chromatography. A Metrohm IC Compact 761 ion chromatograph (IC) was used, equipped with a Metrohm Metrosep A Supp 5 (150/4.0 mm) column, a Metrohm Metrosep A Supp 4/5 Guard pre-column and a conductivity detector. Low molecular weight organic acids were detected and quantified by ultra-high pressure liquid chromatography (UHPLC), consisting of a Phenomenex Rezex Organic Acid H^+ (300x7.8 mm) column, an Ultimate 3000 RS Column Compartiment column oven and an Ultimate 3000 RS Variable Wavelength Detector. Total organic carbon (TOC)

content was measured by a TOC-L CPH analyser equipped with an ASI-L autosampler.

H_2O_2 concentrations were measured using the triiodide method (Klassen et al. 1994).

3. Results and Discussion

3.1 Degradation by LP-UV photolysis

For the overall degradation of a contaminant by LP-UV/H_2O_2 treatment a kinetic model described by Sharpless and Linden (2003), Baeza et al. (2011) and Lester et al. (2010) was applied and is given in the Supplementary Materials.

The degradation of the compounds was found to follow pseudo first-order kinetics for all combinations of UV fluences and H_2O_2 doses. The LP-UV photolysis rate constants ($k_{p,}$ s^{-1}) were derived from the slopes of the regression curves corresponding to LP-UV photolysis and the LP-UV photolysis-hydroxyl radical oxidation combined rate constants (k_T) from those corresponding to the LP-UV/H_2O_2 treatment (Figure 2).

The molar absorption coefficients ($\varepsilon_{C,254}$, M^{-1} cm^{-1}) were measured experimentally and together with the photolysis rate constants ($k_{p,}$ s^{-1}) were used to calculate the quantum yields ($\varphi_{C,254}$, mol/Ein),

following the photochemical approach given by Bolton and Stefan (2002) and using equation (1)

$$k_p = \frac{\varphi_{C,254}\ \varepsilon_{C,254}\ \ln 10}{1000\ U_{\lambda,254}} \qquad (1)$$

where $U_{\lambda,254}$ is the molar photon energy and represents the energy of 1 Ein of photons at 254 nm and is equal to 471528 J/Ein (Bolton and Stefan 2002).

Both the molar absorption coefficient and quantum yield are important parameters, determining the degree of compound degradation by LP-UV photolysis. Although experimentally the highest molar absorption coefficient was obtained for clopyralid (1044 M^{-1} cm^{-1}) compared to mecoprop and metaldehyde (211 and 42 M^{-1} cm^{-1}, respectively), mecoprop was the compound most effectively degraded by LP-UV photolysis at 254 nm, reflecting its greater quantum yield. The quantum yield values that were determined were: for mecoprop 0.8810 mol/Ein, for metaldehyde 0.2014 mol/Ein and for clopyralid 0.0047 mol/Ein (Table 1).

Regarding the very low quantum yield and its difference from the one literature value available given by Autin et al. (2012) (Table 1), this was attributed to the behavior of metaldehyde under LP-UV photolysis, i.e. for the first two UV fluences applied (200 and 400 mJ/cm^2) the degradation increases to approximately 1% and

with higher fluences it subsequently decreases; this phenomenon was observed only for UV photolysis (not for UV/H_2O_2) and also in cases where all pesticides were present in the solution (mixture of the three pesticides).

Mecoprop exhibited the highest degradation ranging from 17% to 60%, since its aromatic structure makes it susceptible to LP-UV photolysis. The degradation was directly proportional to UV fluence.

A very small amount of degradation of clopyralid was observed by LP-UV photolysis (1.2%), despite the presence of a heteroatom (nitrogen) and an aromatic system in its structure. This behaviour could be attributed to the photochemical dissociation mechanism of the pyridine ring; irradiation at 254 nm is thought to cause an n → p* excitation leading to a bicyclic valence isomer, Dewar pyridine, which re-aromatizes completely to pyridine within 15 min at room temperature (Wilzbach and Rausch, 1970).

Degradation of metaldehyde by LP-UV photolysis was negligible (1%). This behaviour was expected due to its low molar absorption coefficient (42 M^{-1} cm^{-1}) and the absence of aromaticity, unsaturated sites or heteroatoms in the molecule.

3.2 Degradation by LP-UV/H_2O_2 treatment

Addition of H_2O_2 caused its photolysis and subsequent production of OH-radicals, non-selective oxidants, enhancing the degradation of all three pesticides. Figure S2 shows the degradation profiles of the three pesticides by LP-UV photolysis and LP-UV/H_2O_2 treatment for all UV fluence/H_2O_2 dose combinations.

LP-UV/H_2O_2 treatment of mecoprop, with a UV fluence as low as 200 mJ/cm^2 and 5 mg/L of H_2O_2, led to a degradation of almost 80%. Under the maximum treatment conditions applied in this research effort (1000 mJ/cm^2 and 15 mg/L H_2O_2) the achieved degradation was 99.6% (2.4-log) (Figure S2). This high reactivity towards OH-attack could be attributed to the presence of the benzene ring substituted with activating groups (-$OCHCH_3COOH$ and –CH_3).

For clopyralid, addition of hydrogen peroxide enhanced the degradation compared to LP-UV photolysis, causing 56% degradation by a UV fluence of 1000 mJ/cm^2 and 5 mg/L H_2O_2. When the H_2O_2 dose was tripled from 5 mg/L to 15 mg/L, a degradation of 84% (0.8-log) was achieved (Figure S2). Of the three pesticides clopyralid was the least susceptible compound to LP-UV/H_2O_2 treatment. This can be explained by the pyridine ring of the molecule, where electrophilic attack is hindered by the low

299 energy of the orbitals of the ring's π-system. In addition, the lone
300 electron pair of the nitrogen atom is not delocalized and
301 destabilizes the cationic 'would-be' intermediate from the
302 electrophilic attack (Clayden et al. 2012).

303 The combination of UV light with hydrogen peroxide was essential
304 for the degradation of metaldehyde due to its non-susceptibility to
305 LP-UV photolysis. LP-UV/H_2O_2 treatment caused a gradual
306 increase of degradation, reaching approximately 1.5-log (97%)
307 degradation for a UV fluence of 1000 mJ/cm^2 and a H_2O_2 dose of
308 15 mg/L (Figure S2). Metaldehyde is a cyclic tetramer of
309 acetaldehyde and an ether derivative. It is proposed that the
310 reaction of OH-radicals with cyclic ethers occurs by direct H atom
311 transfer, in which the hydrogen-bonded adduct formed between the
312 OH-radical and the ether is sterically restricted, leading to a much
313 lower reactivity (Moriarty et al. 2003). Furthermore, the possibility
314 of an H-atom transfer becomes less likely as the ring size
315 increases, due to entropy restrictions (eight-membered-ring in our
316 case).

317 ### 3.3 Kinetics of LP-UV/H_2O_2 treatment

318 Although the pH is expected to affect oxidation processes such as
319 UV/H_2O_2 for the degradation of micropollutants by changing their
320 in the solution, we chose not to buffer for the kinetics-related

experiments. Taking into account the pK_a values for mecoprop (pK_a=3.78) and clopyralid (pK_{a1}=1.4 and pK_{a2}=4.4) (Table S1) and the monitored pH range over which the experiments took place (pH=6.5-7.2), both pesticides are expected to be present in their anionic states. The pH effect would be significant if the pH varied beyond the range below and above the pK_a values; within the range considered in these experiments they are not expected to shift between neutral and ionic state, therefore the kinetics are not expected to be affected. Metaldehyde does not have a pKa value and does not dissociate in water, therefore the pH is not expected to affect its degradation by this process. The photolysis of H_2O_2 is also expected to be favoured at neutral pH, although the greatest enhancement is expected at alkaline pH (Legrini et al. 1993).

The LP-UV photolysis rate constants ($k_{p,}$ s^{-1}) of the pesticides were derived from the slopes of the regression curves given in Figure 2. According to the kinetic rate constants obtained (Table 2) the fastest degradation kinetics by LP-UV photolysis were exhibited by mecoprop ($1.5x10^{-4}$ s^{-1}) followed by metaldehyde ($4.3x10^{-6}$ s^{-1}) and clopyralid ($9.4x10^{-7}$ s^{-1}). When hydrogen peroxide was present the same order of reactivity was observed; for a hydrogen peroxide dose of 15 mg/L, mecoprop exhibited the fastest kinetics ($1.9x10^{-3}$ s^{-1}), followed by metaldehyde ($5.8 x10^{-4}$ s^{-1}) and clopyralid ($3.2x10^{-4}$ s^{-1}). It should be noted that the rate derived for a dose of

344 15 mg/L of hydrogen peroxide was derived on a single datum,
345 since the concentrations of mecoprop for the other UV fluences
346 applied were below the detection limit.

347 The addition of hydrogen peroxide in two different concentrations
348 (5 mg/L and 15 mg/L) had a different impact on the degradation of
349 each pesticide. Mecoprop kinetics were the least affected;
350 compared to LP-UV photolysis a 9-fold and 13-fold increase in
351 kinetic rate constants were observed when 5 mg/L and 15 mg/L of
352 hydrogen peroxide were added, respectively. On the other hand,
353 the rate constants for metaldehyde and clopyralid were strongly
354 enhanced when hydrogen peroxide was added. For metaldehyde,
355 the increase was 74-fold and 134-fold for 5 mg/L and 15 mg/L of
356 peroxide, respectively. Clopyralid exhibited the largest
357 enhancement in terms of kinetic rate constants when hydrogen
358 peroxide was added with a 160-fold and 340-fold increase,
359 respectively. Triplication of the hydrogen peroxide concentration
360 from 5 to 15 mg/L resulted in a 1.4-fold, 1.8-fold and 2-fold
361 increase of the rate constants for mecoprop, metaldehyde and
362 clopyralid, respectively.

363 From a practical point of view, the choice of tripling the H_2O_2
364 depends on the initial influent concentration of the pesticide in a
365 WTW and the level of pesticide degradation desired. In the case of

366 mecoprop, the reaction is fast even at the lowest H_2O_2
367 concentration, with the degradation being enhanced only by around
368 2% when the H_2O_2 concentration is tripled. On the other hand, for
369 metaldehyde and clopyralid, the degradation is enhanced by 11-
370 12%. As an example, an influent concentration of 0.8μg/L
371 metaldehyde treated by a practical UV/H_2O_2 combination of
372 200mJ/cm^2 / 5 mg/L would result in 70% degradation, reducing the
373 concentration to 0.24μg/L, while the permitted level of an
374 individual pesticide in drinking water according to the EU
375 legislation is 0.1μg/L (Council Directive 98/83/EC, 1998).

376 **3.4 Reaction of pesticides with OH-radicals**

377 In order to assess the reactivity of each pesticide towards hydroxyl
378 radicals, the parameters obtained from the single-solute
379 experiments (i.e. the molar absorption coefficients, quantum yields
380 and pseudo first-order rate constants) were incorporated into the
381 UV/H_2O_2 model to obtain the second-order rate constants between
382 each compound and •OH ($k_{\cdot OH/c}$). By combining the equations
383 from the LP-UV/H_2O_2 kinetic model and solving for $k_{\cdot OH/C}$,
384 equation (2) is obtained (Supplementary Materials):

385 $$k_{\cdot OH/C} = \frac{k_{ox}\, k_{\cdot OH,H_2O_2}}{k_{H_2O_2,254}\, \varphi_{H_2O_2,254}} \qquad (2)$$

where k_{ox} (s^{-1}) is the OH-radical oxidation rate constant obtained from the rate constant determined for the UV/H_2O_2 process and corrected for direct photolysis contribution, $k_{.OH,H_2O_2}$ (M^{-1} s^{-1}) is the second-order rate constant for the reaction between hydrogen peroxide and OH-radicals which was assumed to be equal to $2.7x10^7$ M^{-1} s^{-1} (Buxton et al. 1988), $k_{H_2O_2,254}$ (Ein/mol s) is the specific rate of light absorption by hydrogen peroxide at 254 nm, and $\varphi_{H_2O_2,254}$ is the quantum yield of hydrogen peroxide at 254nm (1 mol/Ein).

The values obtained were $3.59x10^8$, $1.96 x10^8$ and $1.09x10^9$ M^{-1} s^{-1} for metaldehyde, clopyralid and mecoprop, respectively (Table 2). From these values it is evident that mecoprop exhibited a substantially greater reactivity towards OH-radicals compared to the other two pesticides (an increase by a factor of 3 and 5.6 compared to metaldehyde and clopyralid, respectively).

Two second-order rate constants are available for metaldehyde and one for clopyralid, whereas for mecoprop more values are available, however with a large variation between them (Table S2). The differences observed between the values obtained in the present study and the ones stated in literature can be attributed to a number of reasons; Apart from the competition kinetics with pCBA, Autin et al. (2012) also utilized the model of Minakata et

al. (2009) where the calculations are based on the molecule geometry and structure. Armbrust et al. (2000) used acetophenone as a reference compound and Beltran et al. (1994) used O_3 or O_3/H_2O_2 as oxidation processes.

The second-order rate constants were also calculated via the competition kinetics with pCBA and the values obtained were $8.3x10^8$, $6.3x10^8$ and $8.9x10^9$ M^{-1} s^{-1} ^{1} for metaldehyde, clopyralid and mecoprop, respectively. The variability for these values was larger as it is shown in Table 2, and also the values themselves were greater for all three pesticides compared to the ones obtained by the kinetic model. This could be attributed to the fact that the method relies on the application of the rate constant of a probe compound, which could be inaccurate, but also to the fact that pCBA is not completely recalcitrant to photolysis (Pereira et al. 2007).

3.5 Reaction product formation

A mechanism for the degradation of each pesticide under LP-UV photolysis combined with OH-attack (and also of LP-UV photolysis in the case of mecoprop) was proposed. The identification of the reaction products was mainly based on the structural information obtained from the fragmentation patterns of the mass spectrometry applied, in combination with the hydroxyl

radical chemistry. In our case OH-radical attack followed two main mechanisms; 1) H-atom abstraction from a C-H bond by •OH reactions; 2) electrophilic substitution by the •OH, in cases of double bonds and aromatic systems. Groups attached to the aromatic rings can either activate or deactivate the aromatic ring towards electrophilic substitution (Clayden et al. 2012).

The double-bond-equivalents (DBE) parameter was also used to determine unknown structures. DBE is a well-established tool in mass spectrometry that determines the summation of the unsaturations plus rings in a molecule, calculated via a specific molecular formula (Nassar and Talaat, 2004). The verification of the final structure is possible in combination with the use of NMR, IR spectroscopy and mass spectrometry (only the latter applied in our case). Starting from the parent compound, the DBE was calculated for all the possible molecular structures of the products detected, and the most likely structure for each product was suggested. In cases where the molecular structures resulted either in a negative or fraction DBE values (which is not possible since DBE has to be a positive integer) or the respective structures would not match the oxidation pathways expected from the OH-attack, the molecular structure was rejected. Following this process for all products detected for all three pesticides, the structure elucidation process was facilitated.

453 The main photo-product of LP-UV photolysis of mecoprop, 2-(4-
454 hydroxy-2-methylphenoxy)propanoic acid (Product I, m/z=196),
455 was produced via photo-hydrolysis of the chlorine atom on the
456 benzene ring (Figure S3). This product had the highest peak area in
457 the chromatograms and increased with increasing UV fluence. It
458 was also produced by LP-UV/H_2O_2 treatment but with a smaller
459 area, decreasing at UV fluences higher than 1000 mJ/cm^2. This
460 product has also been reported as the main photo-product by UV
461 photolysis at 254nm, by Meunier and Boule (2000) and Boule et
462 al. (2002). Subsequent OH-attack on the tertiary carbon atom of
463 the propanoic moiety led to H-abstraction and carbon-centered
464 radical formation, which reacted with oxygen and formed 2-
465 methylhydroquinone (Product II, m/z=124) and pyruvic acid
466 (Product III, m/z=88). Direct OH-attack on the tertiary carbon
467 atom of the propanoic moiety of mecoprop led to 2-methyl-4-
468 chlorophenol (Product IV, m/z=142) and pyruvic acid. A product
469 with an m/z of 108 suggests formation of 2-cresol (Product V),
470 although radical-radical reactions in aquatic solution are very
471 unlikely. Another possibility would be the reduction by the
472 hydroperoxyl radical ($HO_2^{\bullet}$) formed by photolysis of hydrogen
473 peroxide. The formation of this product in small concentrations by
474 direct LP-UV photolysis has been reported before, while the rest of
475 the products mentioned have also been observed after either UV

476 photolysis or UV/TiO_2 oxidation (Topalov et al. 1999, Meunier
477 and Boule 2000, Boule et al. 2002). De-chlorination of the
478 molecule was confirmed by the formation of chloride ion; 94% of
479 the organic chlorine was converted into chloride ion after three
480 hours of irradiation (UV fluence 1500 mJ/cm^2) with 30 mg/L H_2O_2
481 (Figure S4a) with a chloride ion concentration in the solution up to
482 1.5 mg/L. Products from electrophilic substitution of the aromatic
483 ring were not observed, suggesting that this mechanism is not
484 favoured. Figure 3 shows the degradation of mecoprop (10 mg/L)
485 and the reaction product formation as a function of the UV fluence
486 for a H_2O_2 dose of 30 mg/L. The proposed degradation pathways
487 for mecoprop are shown in Figure 4.

488 The degradation of clopyralid by LP-UV/H_2O_2 treatment (Figure
489 5) yielded two main reaction products, 3,6-dichloro-4-
490 hydroxypyridine-2-carboxylic acid and 3,6-dichloro-5-
491 hydroxypyridine-2-carboxylic acid (Products I, m/z=208 for both
492 structures) by OH-attack onto one of the two available carbon
493 atoms of the pyridine ring, causing H-abstraction and carbon-
494 centered radical formation, which after reacting with oxygen
495 yielded the mentioned product. 3,6-dichloro-5-hydroxypyridine-2-
496 carboxylic acid was the main product, in agreement with the
497 directing and activating effects of the substituents of the ring
498 (Clayden et al. 2012). These two products have been reported as

well for clopyralid oxidation by MP-UV/TiO_2 oxidation (Sojic et al., 2009). A peak of m/z=164, probably 3,6-dichloro-pyridin-2-ol (Product II), was observed at a UV fluence of 500 mJ/cm^2, slowly decreasing with increasing UV fluence; this compound was identified also by Sojic et al. (2009). However, formation of this compound is theoretically unlikely, since it suggests radical-radical reactions. Finally, a chloro-hydroxypyridine carboxylic acid with m/z=174 was observed (Product III) with the largest peak area at a UV fluence of 500 mJ/cm^2, followed by degradation at increasing UV fluence. This product may have been formed by de-chlorination and OH-radical substitution on one of the two chlorine-bearing carbon atoms of the pyridine ring. Figure 5 shows the degradation of clopyralid (20mg/L) and the reaction product formation as a function of the UV fluence for a H_2O_2 dose of 60 mg/L. The de-chlorination of the molecule was supported by the increasing chloride concentration in the solution. The chloride concentration increased with increasing UV and H_2O_2 doses and the conversion of organic chlorine to chloride ion reached 64% (4.7 mg/L Cl^- released) at a fluence of 1500 mJ/cm^2 with 60 mg/L H_2O_2 (Figure S4b). De-chlorination products were also found in the case of clopyralid treatment by MP-UV/H_2O_2 treatment (Xu et al., 2013). The proposed degradation pathways for mecoprop are shown in Figure 6.

The degradation of metaldehyde by LP-UV/H_2O_2 treatment yielded quite a different set of reaction products compared to the other two pesticides, since the molecule is a cyclic polyether lacking aromaticity. The two main reaction products with m/z 210 and 226 were detected twice, suggesting that two isomers with the same molecular weight were formed for each m/z observed. The formation profile for the m/z 210 product can be seen in Figure S5, and the same profile was found for the m/z 226 product. The main products observed for the degradation of metaldehyde (Figure 7) suggest successive reactions that could be supported by the following mechanism: Metaldehyde becomes hydroxylated once (m/z=210) or twice (m/z=226) via OH-attack on the tertiary carbon atoms of the ring. Due to the analytical detection method (positive mode detection with NH_4^+) formation of a complex via hydrogen bonding between the oxygen atoms of the hydroxylated molecule and the NH_4^+ group, similarly to a crown ether took place (Hurtado et al. 2012). These products exhibited specific fragmentation with the production of a fragment with m/z=62 identified as the $[CH_3\dot{C}HO\text{---}H\text{-}NH_3]$ complex. This complex suggests the formation of acetaldehyde, which was the main expected product. Since carbonyl compounds could not be detected with our method, acetaldehyde was not detected directly. Acetaldehyde formation was also supported by the detection of acetic acid as an end

545 product at UV fluences higher than 500 mJ/cm^2 (Figure S6). De-
546 protonation from the ring followed by OO· addition (Auzmendi-
547 Murua and Bozzelli, 2014) could lead to formation of a molecule
548 with a keto-ether on the one end and an oxyl radical on the other,
549 whereas de-protonation of the methyl groups (less likely) would
550 lead to demethylation.

551 Little mineralization was observed during the LP-UV/H_2O_2
552 treatment of the studied pesticides. The TOC levels for mecoprop
553 and metaldehyde exhibited a small decrease under the conditions
554 applied; the maximum TOC reductions observed under the
555 maximum UV fluence and H_2O_2 doses were 21% and 17%,
556 respectively. For clopyralid the TOC content in the solution
557 showed a gradual decrease with increasing UV fluence and H_2O_2
558 dose, and reached a maximum TOC reduction of 34% under the
559 highest UV/H_2O_2 doses, applied in this research effort.

560 ### 3.6 Relevance for practice

561 Based on the findings of this research, it can be concluded that LP-
562 UV/H_2O_2 treatment can be a suitable process for the degradation of
563 the three pesticides studied. Assuming that their influent
564 concentrations are in the typical hundreds ng/L to a few μg/L, the
565 average LP-UV/H_2O_2 conditions can degrade them sufficiently; in
566 cases of higher influent levels, the desired degradation can be

567 achieved by an increase of the doses whilst still remaining within
568 practical ranges (UV fluences up to 1000mJ/cm^2 and H_2O_2 up to
569 15 mg/L).

570 Regarding the significance of the reaction products identified,
571 toxicity information is available only for 2-cresol. The EPA (IRIS)
572 has classified 2-cresol as a possible human carcinogen
573 (Classification C) based on an increased incidence of skin
574 papillomas in mice in an initiation-promotion study (U.S.EPA,
575 2014). However, in water treatment the low molecular weight
576 compounds usually produced by oxidation processes are expected
577 to be biodegraded and/or adsorbed by post treatment processes (eg.
578 granular activated carbon filtration).

579 There are only a few studies of pesticide treatment by LP-
580 UV/H_2O_2 treatment that discuss toxicity effects (Linden et al. 2004,
581 Lekkerkerker- Teunissen et al, 2013, Choi et al. 2013, Mariani et
582 al. 2015), as well as a few considering toxicity of medium pressure
583 UV treatment (Kruithof et al. 2007, Heringa et al. 2011, Martijn
584 and Kruithof 2012). These have generally indicated less
585 genotoxicity formation by low pressure compared to medium
586 pressure UV applications. Nevertheless, toxicity testing after LP-
587 UV/H_2O_2 treatment should be performed to establish whether there
588 are reasons for concern.

589 Recent research suggests that background water components (e.g.
590 nitrate and natural organic matter) may play a more important role
591 in toxicity formation by UV/H_2O_2 treatment than the target
592 micropollutants (Martijn and Kruithof 2012, Martijn et al. 2015,
593 Parkinson et al. 2011) and greater attention should be given to this
594 in future studies.

595 ## 4. Conclusions

596 The main conclusions from the results of this study can be
597 summarized as follows:

598 • The order of degradation observed by both LP-UV
599 photolysis and UV/H_2O_2 treatment was the following:
600 mecoprop>metaldehyde>clopyralid; the rate constants by
601 LP-UV photolysis were $1.5x10^{-4}$, $4.3x10^{-6}$ and $9.4x10^{-7}$ s^{-1},
602 respectively. For 15 mg/L H_2O_2, the rate constants
603 increased to $1.9x10^{-3}$, 5.8 $x10^{-4}$ and $3.2x10^{-4}$ s^{-1},
604 respectively. Clopyralid exhibited the largest enhancement
605 in kinetic rate terms after H_2O_2 addition. The second-order
606 rate constants for the reaction of the pesticides with OH-
607 radicals ($k_{\cdot OH/C}$) were calculated via kinetic modeling as
608 $1.1x10^{9}$, $3.3x10^{8}$, $2.0x10^{8}$ M^{-1} s^{-1} and via competition

kinetics as $8.9x10^9$, $8.3x10^8$ and $6.3x10^8$ M^{-1} s^{-1} for mecoprop, metaldehyde and clopyralid, respectively.

- Mecoprop underwent photo-hydrolysis by LP-UV photolysis yielding one main photo-product (2-(4-hydroxy-2-methylphenoxy)propanoic acid) while several other products being formed from either the oxidation of the benzene ring or of the side chain were formed when LP-UV/H_2O_2 treatment was applied. Clopyralid generated products mainly via either hydroxylation or dechlorination of the pyridine ring. Metaldehyde was hydroxylated via OH-radical attack. The intermediates, such as acetaldehyde, formed NH_4^+-complexes due to the detection method. Further degradation to acetic acid was observed.

Acknowledgements

This work was performed in the cooperation framework of Wetsus, European Centre of Excellence for Sustainable Water Technology (www.wetsus.eu). Wetsus is co-funded by the Dutch Ministry of Economic Affairs and Ministry of Infrastructure and Environment, the Province of Fryslân and the Northern Netherlands Provinces. The authors like to thank the participants of the research theme Priority Compounds for the fruitful discussions and their financial support. Specifically the authors gratefully acknowledge the

631 financial support by Anglian Water Services Ltd., Trojan
632 Technologies Inc. for supplying the low pressure UV lamp,
633 Mihaela I. Stefan for the fruitful discussions on photochemistry
634 and the laboratory staff of Wetsus Institute, and especially Ton van
635 der Zande for the realization of the instrumental analysis.

636 **Nomenclature**

Symbol	Quantity name	Dimension
k_p	photolysis rate constant	s^{-1}
$\varepsilon_{C,254}$	molar absorption coefficient of a compound at 254 nm	M^{-1} cm^{-1}
$\varphi_{C,254}$	quantum yield of a compound at 254 nm	mol/Ein
$U_{\lambda,254}$	the molar photon energy at 254 nm	J/Ein
$k_{\bullet OH/C}$	rate constant between a compound and OH-radicals	M^{-1} s^{-1}
k_{ox}	OH-radical oxidation rate constant	s^{-1}
$k_{\bullet OH,H_2O_2}$	rate constant between hydrogen	M^{-1} s^{-1}

	peroxide and OH-radicals	
$k_{H_2O_2,254}$	specific rate of light absorption of hydrogen peroxide at 254 nm	Ein/mol s
$\varphi_{H_2O_2,254}$	quantum yield of hydrogen peroxide at 254 nm	mol/Ein

637

638 ## References

639 Armbrust K.L., 2000. Pesticide hydroxyl radical rate constants:
640 Measurements and estimates of their importance in aquatic
641 environments. Environmental Toxicology and Chemistry, 19 (9),
642 2175–2180.

643 Autin O., Hart J., Jarvis P., MacAdam J., Parsons S. A., Jefferson
644 B., 2012. Comparison of UV/ H_2O_2 and UV/TiO_2 for the
645 degradation of metaldehyde: Kinetics and the impact of
646 background organics. Water Research, 46 (17), 5655-5662.

647 Autin O., Hart J., Jarvis P., MacAdam J., Parsons S. A., Jefferson
648 B., 2013. The impact of background organic matter and alkalinity
649 on the degradation of the pesticide metaldehyde by two advanced

650 oxidation processes: UV/ H_2O_2 and UV/TiO_2. Water Research, 47
651 (6), 2041-2049.

652 Auzmendi-Murua I. and Bozzelli J.W., 2014. Thermochemical
653 Properties and Bond Dissociation Enthalpies of 3- to 5‑Member
654 Ring Cyclic Ether Hydroperoxides, Alcohols, and Peroxy
655 Radicals: Cyclic Ether Radical + $^3O_2$ Reaction Thermochemistry.
656 The Journal of Physical Chemistry A, 118 (17), 3147–3167.

657 Baeza, C., Knappe, D.R.U., 2011. Transformation kinetics of
658 biochemically active compounds in low-pressure UV Photolysis
659 and UV/H_2O_2 advanced oxidation processes. Water Research, 45
660 (15), 4531-4543.

661 Bolton, J. R., Stefan M. I., 2002. Fundamental photochemical
662 approach to the concepts of fluence (UV dose) and electrical
663 energy efficiency in photochemical degradation reactions.
664 Research on Chemical Intermediates, 28 (7-9), 857–870.

665 Bolton, J. R., Linden K.G., 2003. Standardization of Methods for
666 Fluence (UV Dose) Determination in Bench-Scale UV
667 Experiments. Journal of Environmental Engineering, 29 (3), 209–
668 215.

669 Boule P., Meunier L., Bonnemoy F., Boulkamh A., Zertal A,
670 Lavedrine B., 2002. Direct phototransformation of aromatic

671 pesticides in aqueous solution. International Journal of
672 Photoenergy, 4 (2), 69-78.

673 Buxton G.V., Greenstock C.L., Helman W.P., Ross A.B. 1988.
674 Critical review of rate constants for reactions of hydrated electrons,
675 hydrogen atom and hydroxyl radicals (OH/O-) in aqueous
676 solutions. J. Phys. Chem. Ref. Data, 17, 513–886.

677 Choi H-J, Kim D., Lee T-J, 2013. Photochemical degradation of
678 atrazine in UV and UV/H_2O_2 process: pathways and toxic effects
679 of products. Journal of Environmental Science and Health, Part B:
680 Pesticides, Food Contaminants, and Agricultural Wastes, 48 (11),
681 927–934.

682 Clayden J., Greeves N., Warren S., Wothers P., 2012. Organic
683 Chemistry, 2nd Edition, 544-568, 1149-1153. Oxford University
684 Press, USA.

685 Cooper B, 2011. Working with farmers to reduce pesticide
686 movement to water. Aspects of Applied Biology, 106, 289-294.
687 Crop Protection in Southern Britain.

688 Council Directive 98/83/EC of 3 November 1998 on the quality of
689 water intended for human consumption [2003] OJ L330/32.

690 Donald D.B., Cessna A.J, Sverko E., Glozier N.E., 2007.
691 Pesticides in Surface Drinking-Water Supplies of the Northern
692 Great Plains. Environmental Health Perspectives, 15 (8), 1183-
693 1191.

694 Gill H.K., Garg H., 2014. Pesticides: Environmental Impacts and
695 Management Strategies, Pesticides - Toxic Aspects, Dr. Sonia
696 Soloneski (Ed.), ISBN: 978-953-51-1217-4, InTech. DOI:
697 10.5772/57399.

698 Heringa M.B., Harmsen D.J.H., Beerendonk E.F., Reus A.A., Krul
699 C.A.M., Metz D.H., IJpelaar G.F., 2011. Formation and removal of
700 genotoxic activity during UV/H_2O_2-GAC treatment of drinking
701 water. Water Research, 45 (1), 366-374.

702 Hurtado P., Gámez F., Hamad S., Martínez–Haya B., Steill J.D.,
703 Oomens J., 2012. Multipodal coordination of a tetracarboxylic
704 crown ether with NH_4^+: A vibrational spectroscopy and
705 computational study. The Journal of Chemical Physics, 136 (11),
706 114301-1 – 114301-6.

707 Klassen N.V., Marchington D., McGowan H.C.E., 1994. H_2O_2
708 Determination by the I_3^- Method and by $KMnO_4$ Titration.
709 Analytical Chemistry, 66 (18), 2921–2925.

710 Kruithof J.C., Kamp P.C., Martijn B.J., 2007. UV/H_2O_2 Treatment:
711 A Practical Solution for Organic Contaminant Control and Primary
712 Disinfection. Ozone: Science & Engineering, 29 (4), 273–280.

713 Legrini O., Oliveros E., Braun A.M., 1993. Photochemical
714 Processes for Water Treatment. Chemical Reviews, 93 (2), 671–
715 698

716 Lekkerkerker-Teunissen K., Knol A.H., Derks J.G., Heringa M.B.,
717 Houtman C.J., Hofman-Caris C.H.M., Beerendonk E.F., Reus A.,
718 Verberk J.Q.J.C., van Dijk J.C., 2013. Pilot Plant Results with
719 Three Different Types of UV Lamps for Advanced Oxidation.
720 Ozone: Science & Engineering, 35 (1), 38–48.

721 Lester Y., Avisar D., Mamane H., 2010. Photodegradation of the
722 antibiotic sulphamethoxazole in water with UV/H_2O_2 advanced
723 oxidation process. Environmental Technology, 31 (2), 175–183.

724 Linden, K.G., Rosenfeldt, E.J., Chen, P.J., Kullman, S.W., 2004.
725 UV and UV/H_2O_2 degradation and subsequent toxicity of
726 endocrine disrupting chemicals in water. European Conference on
727 UV Radiation, Karlsruhe, Germany.

728 Martijn B.J. , Kruithof J.C., 2012. UV and UV/H_2O_2 Treatment:
729 The Silver Bullet for By-product and Genotoxicity Formation in
730 Water Production. Ozone: Science & Engineering, 34 (2), 92–100.

731 Martijn B.J. , Kruithof J.C., Hughes R.M., Mastan R.A., van
732 Rompay A.R.., Malley J.P.Jr., 2015. Induced Genotoxicity in
733 Nitrate-Rich Water Treated With Medium-Pressure Ultraviolet
734 Processes. American Water Works Association, 107 (6), E301-
735 E312.

736 Melisa L. Mariani,a Roberto L. Romeroa and Cristina S. Zalazar,
737 2015. Modeling of degradation kinetic and toxicity evaluation of
738 herbicides mixtures in water using the UV/H_2O_2 process.
739 Photochemical & Photobiological Sciences, 14 (3), 608–617.

740 Meunier L., Boule P., 2000. Direct and induced
741 phototransformation of mecoprop [2-(4-chloro-2-methylphenoxy)-
742 propionic acid] in aqueous solution. Pest Management Science, 56
743 (12), 1077-1085.

744 Minakata D., Li K., Westerhoff P., Crittenden J., 2009.
745 Development of a Group Contribution Method To Predict Aqueous
746 Phase Hydroxyl Radical (HO•) Reaction Rate Constants.
747 Environmental Science and Technology, 43 (16), 6220-6227.

748 Moriarty J., Sidebottom H., Wenger J., Mellouki A., Le Bras G.,
749 2003. Kinetic Studies on the Reactions of Hydroxyl Radicals with
750 Cyclic Ethers and Aliphatic Diethers. The Journal of Physical
751 Chemistry, 107 (10), 1499-1505.

752 Nassar A-E. F., Talaat R.E., 2004. Strategies for dealing with
753 metabolite elucidation in drug discovery and development. Drug
754 Discovery Today, 9 (7), 317-327.

755 Orellana-García F., Álvarez M.A., López-Ramón V., Rivera-
756 Utrilla J., Sánchez-Polo M., Mota A.J., 2014. Photodegradation of
757 herbicides with different chemical natures in aqueous solution by
758 ultraviolet radiation. Effects of operational variables and solution
759 chemistry. Chemical Engineering Journal 255 (1), 307–315.

760 Parkinson A, Barry M.J., Roddick F.A., Hobday M.D., 200.
761 Preliminary Toxicity Assessment of Water after Treatment with
762 UV-Irradiation and UVC/H_2O_2. Water Research, 35(15), 3656-
763 3664.

764 Pereira V.J., Weinberg H.S., Linden K.G., Singer P.C., 2007. UV
765 Degradation Kinetics and Modeling of Pharmaceutical Compounds
766 in Laboratory Grade and Surface Water via Direct and Indirect
767 Photolysis at 254 nm. Environmental Science & Technology, 1 (5),
768 1682–1688.

769 Pi Y., Schumacher J., Jekel M., 2005. The Use of para-
770 Chlorobenzoic Acid (pCBA) as an Ozone/Hydroxyl Radical Probe
771 Compound. Ozone: Science and Engineering, 27 (6), 431–436.

772 Sharpless C. M., Linden K.G., 2003. Experimental and Model
773 Comparisons of Low- and Medium-Pressure Hg Lamps for the
774 Direct and H_2O_2 Assisted UV Photodegradation of N-
775 Nitrosodimethylamine in Simulated Drinking Water.
776 Environmental Science and Technology, 37 (9), 1933-1940.

777 Šojić D.V., Anderluh V.B., Orčić D. Z., Abramović B. F., 2009.
778 Photodegradation of clopyralid in TiO_2 suspensions: Identification
779 of intermediates and reaction pathways. Journal of Hazardous
780 Materials, 168 (1), 94-101.

781 Stuart M.E., Manamsa k., Talbot J.C., Crane E.J., 2011. Emerging
782 contaminants in groundwater. British Geological Survey. Natural
783 Environment Research Council. Keyworth, Nottingham

784 Swaim P., Royce A., Smith T. , Maloney T., Ehlen D., Carter B.,
785 2008. Effectiveness of UV Advanced Oxidation for Destruction of
786 Micro-Pollutants. Ozone: Science and Engineering, 30 (1), 34–42.

787 Tizaoui C., Mezughi K., Bickley R., 2011. Heterogeneous
788 photocatalytic removal of the herbicide clopyralid and its
789 comparison with UV/ H_2O_2 and ozone oxidation techniques.
790 Desalination 273 (1), 197–204.

791 Topalov A., Molnár-Gábor D., Kosanić M., Abramović B., 1999.
792 Photomineralization of the herbicide mecoprop dissolved in water
793 sensitized by TiO_2. Water Research, 34 (5), 1473-1478.

794 Vilhunen S., Sillanpää M., 2010. Recent developments in
795 photochemical and chemical AOPs in water treatment: a mini-
796 review. Reviews in Environmental Science and Bio/Technology, 9
797 (4), 323-330.

798 Wilzbach K. E., Rausch D. J., 1970. Photochemistry of Nitrogen
799 Heterocycles. Dewar Pyridine and Its Intermediacy in
800 Photoreduction and Photohydration of Pyridine. Journal of the
801 American Chemical Society, 92 (7), 2178-2179.

802 Xu G., Liu N., Wu M., Bu T., Zheng M., 2013. The
803 Photodegradation of Clopyralid in Aqueous Solutions: Effects of
804 Light Sources and Water Constituents. Industrial & Engineering
805 Chemistry Research, 52 (29), 9770-9774.

806 ## Web References

807 Drinking Water Inspectorate, 2015. Annual report. Last accessed
808 on 08/09/2015. Retrieved from www.dwi.gov.uk

University of Hertfordshire, 2015. PPDB: Pesticide Properties DataBase, mecoprop. Last accessed on 06/09/2015. Retrieved from http://sitem.herts.ac.uk/aeru/ppdb/en/Reports/430.htm

U.S. EPA, 2014. Integrated Risk Information System, 2-Methylphenol (CASRN 95-48-7). Last accessed on 06/09/2015. Retrieved from http://www.epa.gov/iris/subst/0300.htm#carc

Tables

Table 1. Molar absorption coefficient ($\varepsilon_{C,254}$) and quantum yield ($\phi_{C,254}$) values derived from this study and reported in literature (values from duplicates given in brackets in case they differed).

	This study		Literature	
Compound	**$\varepsilon_{C,254}$ (M^{-1} cm^{-1})**	**$\varphi_{C,254}$ (mol/Ein)**	**$\varepsilon_{C,254}$ (M^{-1} cm^{-1})**	**$\varphi_{C,254}$ (mol/Ein)**
Metaldehyde	42.11 (42.06-42.17)	0.2014 (0.1938 – 0.2090)	21.4 [2], 19.6 [3]	0.000017 [2], 0.00020 [3]
Clopyralid	1044 (998.1-1090)	0.0047 (0.0036 – 0.0059)	845 [4]	0.068 [4]
Mecoprop	210.7	0.8810	244 [5]	0.75 [6], 0.34

[2] Autin et al. (2012)
[3] Autin et al. (2013)
[4] Orellana-Garcia et al. (2014)
[5] Estimated from Fig.1 of Meunier and Boule (2000)

	(203.4-218.1	(0.8474 – 0.9145)	[7] 0.23 [8]

[6] Meunier and Boule (2000) (λ=280nm, pH 5.5, +/- O_2)
[7] Meunier and Boule (2000) (λ=280nm, pH 2.15, O_2)
[8] Meunier and Boule (2000) (λ=280nm, pH 2.15, -O_2)

819 Table 2. Time-based pseudo first-order rate constants for UV photolysis and UV/H_2O_2 oxidation (k_p, k_T, s^{-1}) for the three pesticides
820 (values from duplicates given in brackets in case they differed).

Compound	**k_p (photolysis)**	**k_T (photolysis + •OH)**		**$k•_{OH/C}$ (kinetic modeling)**	**$k•_{OH/C}$ (pCBA kinetics)**
	(s^{-1})	**(s^{-1})**		**(M^{-1} s^{-1})**	**(M^{-1} s^{-1})**
	No H_2O_2	**UV + 5 mg/L H_2O_2**	**UV + 15 mg/L H_2O_2**	-	-
Metaldehyde	$4.3x10^{-6}$ [$7.5x10^{-6}$ – $1.0x10^{-6}$]	$3.2x10^{-4}$ [$2.9x10^{-4}$– $3.5x10^{-4}$]	$5.8x10^{-4}$ [$5.6x10^{-4}$– $6.0x10^{-4}$]	$3.6x10^{8}$ [$3.3x10^{8}$- $3.9x10^{8}$]	$8.3x10^{8}$ [$7.0x10^{8}$-$9.8x10^{8}$]
Clopyralid	$9.4x10^{-7}$	$1.5x10^{-4}$	$3.2x10^{-4}$ [$3.4\ x10^{-4}$ – $3.1x10^{-4}$]	$2.0x10^{8}$	$6.3x10^{8}$ [$5.0x10^{8}$-$7.5x10^{8}$]

Mecoprop	$1.5x10^{-4}$	$1.4x10^{-3}$	$1.9x10^{-3}$	$1.1x10^{9}$ [$1.11x10^{9}$- $1.08x10^{9}$]	$8.9x10^{9}$ [$8.6x10^{9}$-$9.3x10^{9}$]

821

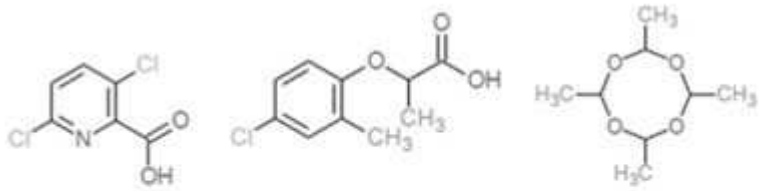

Clopyralid **Mecoprop** **Metaldehyde**

Figure 1. Chemical structure of the studied pesticides

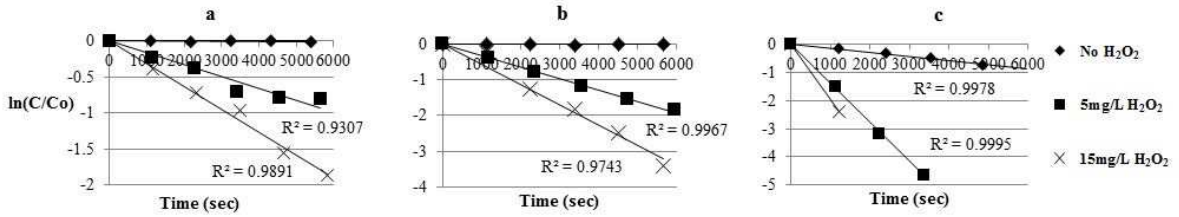

Figure 2. Degradation kinetics (used for the determination of the pseudo first-order rate constants) of (a) clopyralid, (b) metaldehyde and (c) mecoprop, by low pressure UV photolysis (no H_2O_2) and UV/H_2O_2 treatment.

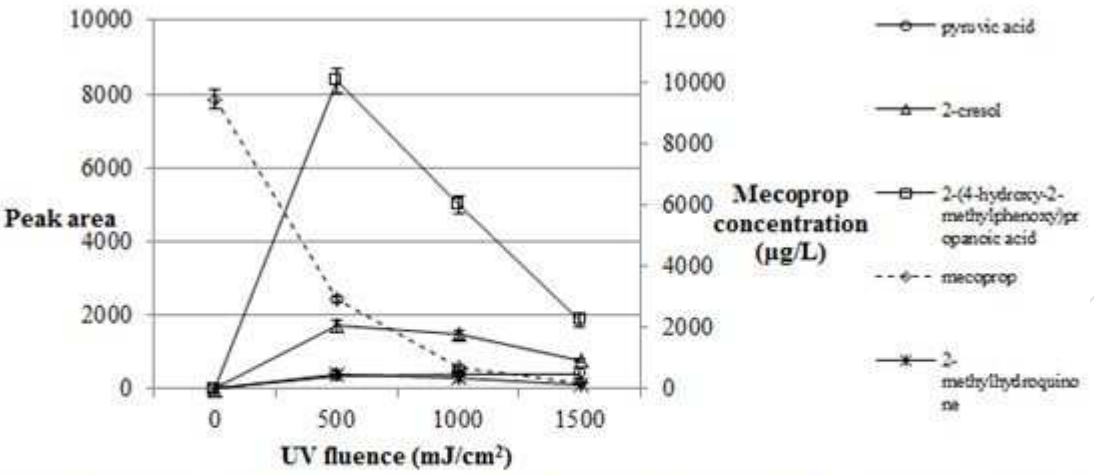

Figure 3. Mecoprop (10 mg/L) degradation and reaction product formation as a function of the UV fluence (30 mg/L H_2O_2; secondary vertical axis refers to the concentration of mecoprop (dashed line)).

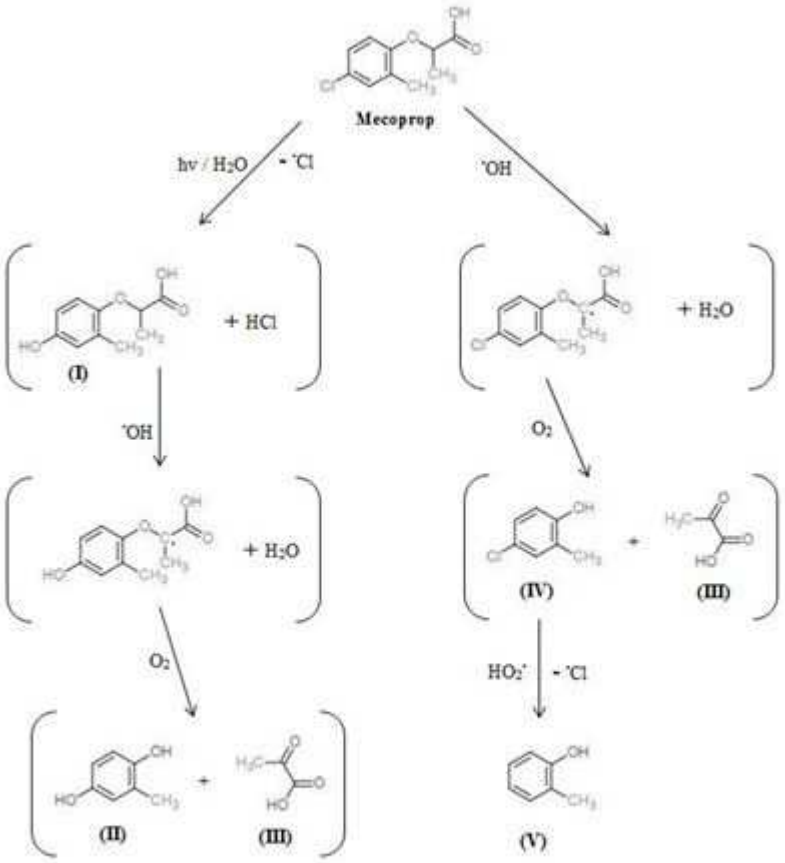

Figure 4. Proposed pathways for mecoprop degradation by UV/H_2O_2 treatment.

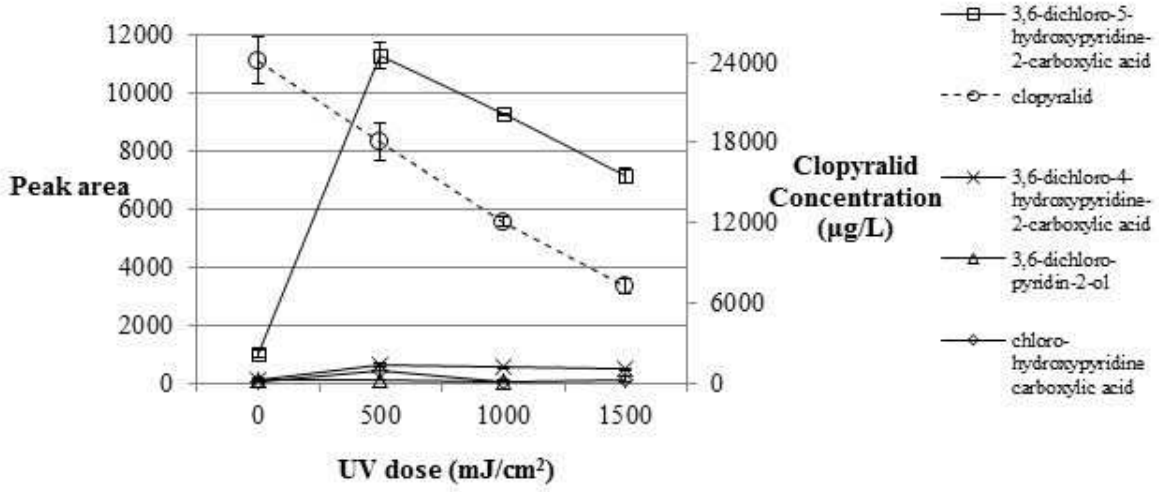

Figure 5. Clopyralid (20 mg/L) degradation and reaction product formation as a function of the UV fluence (60 mg/L H_2O_2; secondary vertical axis refers to the concentration of clopyralid (dashed line)). Error bars represent the standard deviation for duplicate measurements.

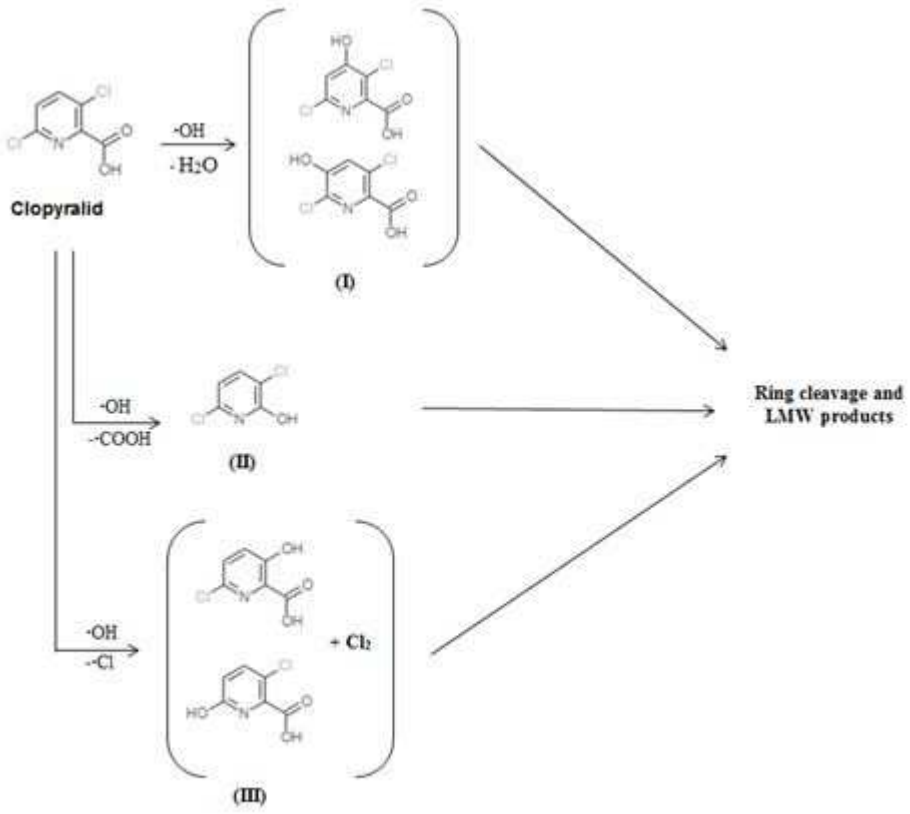

Figure 6. Proposed pathways for clopyralid degradation by UV/H_2O_2 treatment.

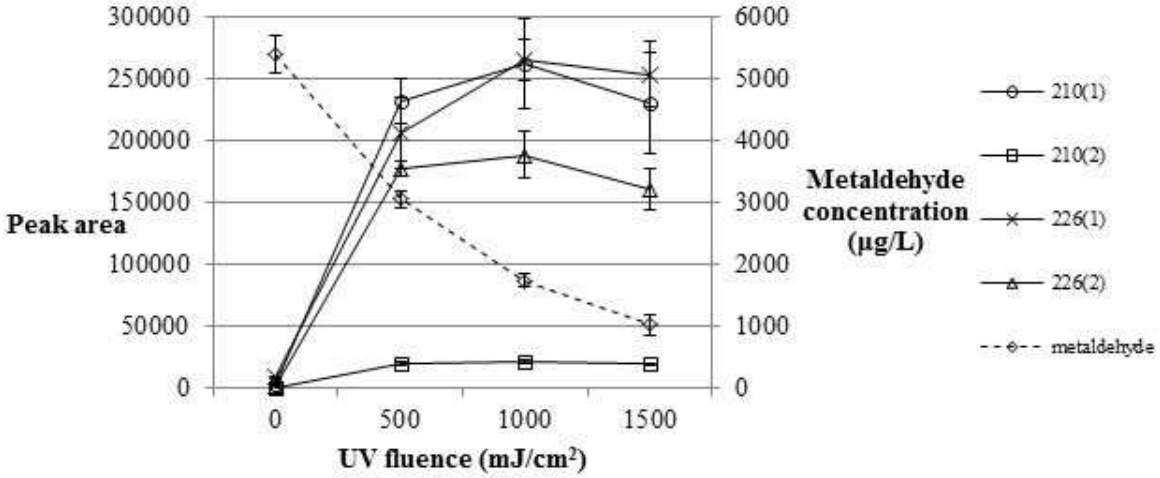

Figure 7. Metaldehyde (5 mg/L) degradation and reaction product formation as a function of the UV fluence (30 mg/L H_2O_2; secondary vertical axis refers to the concentration of metaldehyde (dashed line)). Error bars represent the standard deviation for duplicate measurements.

- The degradation order observed for LP-UV/H_2O_2 was mecoprop>metaldehyde>clopyralid.
- The same degradation order was observed for the reaction with the OH-radicals.
- Clopyralid exhibited the largest enhancement in kinetics with H_2O_2 addition.
- Mecoprop produced one photolysis product and smaller ones from OH-radical attack.
- Clopyralid and metaldehyde produced mainly hydroxylated products.